Neotectonic and Paleoseismic Onshore-Offshore integrated study of the Carboneras Fault (Eastern Betics, SE Iberia)

Estudio integrado tierra-mar de la Neotectonica y Paleosismología de la Falla de Carboneras (Béticas Orientales, SE Península Ibérica)

Ximena Moreno Mota

ADVERTIMENT. La consulta d'aquesta tesi queda condicionada a l'acceptació de les següents condicions d'ús: La difusió d'aquesta tesi per mitjà del servei TDX (**www.tdx.cat**) ha estat autoritzada pels titulars dels drets de propietat intel·lectual únicament per a usos privats emmarcats en activitats d'investigació i docència. No s'autoritza la seva reproducció amb finalitats de lucre ni la seva difusió i posada a disposició des d'un lloc aliè al servei TDX. No s'autoritza la presentació del seu contingut en una finestra o marc aliè a TDX (framing). Aquesta reserva de drets afecta tant al resum de presentació de la tesi com als seus continguts. En la utilització o cita de parts de la tesi és obligat indicar el nom de la persona autora.

ADVERTENCIA. La consulta de esta tesis queda condicionada a la aceptación de las siguientes condiciones de uso: La difusión de esta tesis por medio del servicio TDR (**www.tdx.cat**) ha sido autorizada por los titulares de los derechos de propiedad intelectual únicamente para usos privados enmarcados en actividades de investigación y docencia. No se autoriza su reproducción con finalidades de lucro ni su difusión y puesta a disposición desde un sitio ajeno al servicio TDR. No se autoriza la presentación de su contenido en una ventana o marco ajeno a TDR (framing). Esta reserva de derechos afecta tanto al resumen de presentación de la tesis como a sus contenidos. En la utilización o cita de partes de la tesis es obligado indicar el nombre de la persona autora.

WARNING. On having consulted this thesis you're accepting the following use conditions: Spreading this thesis by the TDX (**www.tdx.cat**) service has been authorized by the titular of the intellectual property rights only for private uses placed in investigation and teaching activities. Reproduction with lucrative aims is not authorized neither its spreading and availability from a site foreign to the TDX service. Introducing its content in a window or frame foreign to the TDX service is not authorized (framing). This rights affect to the presentation summary of the thesis as well as to its contents. In the using or citation of parts of the thesis it's obliged to indicate the name of the author.

RISKNAT
Departament de Geodinàmica i Geofísica
Universitat de Barcelona

Barcelona Center for Subsurface Imaging
Unidad de tecnología Marina
Consejo Superior de Investigaciones Científicas

Neotectonic and Paleoseismic Onshore-Offshore integrated study of the Carboneras Fault (Eastern Betics, SE Iberia)

Estudio integrado tierra-mar de la Neotectonica y Paleosismología de la Falla de Carboneras (Béticas Orientales, SE Península Ibérica)

Memoria presentada por

Ximena Moreno Mota

para optar al grado de Doctora en Geología

Esta memoria se ha realizado dentro del programa de Ciències de la Terra (bienio 2005-2006) de la Universitat de Barcelona bajo la dirección de las Doctoras Eulàlia Masana Closa y Eulàlia Gràcia Mont

Barcelona, Julio de 2010

Part IV: Discussion and conclusions

Chapter 8: Discussion. Onshore-offshore integration of the results

8.1. Neotectonics of the Carboneras Fault Zone

8.1.1. Activity of the CFZ: From the Miocene to the Present day

In the Almería Margin, the Carboneras Fault Zone (CFZ) was observed in seismic profiles as a basement high bounded by faults and delimiting Miocene sub-basins on each side (Fig. 6.14, 6.15, 6.18, 6.19, 6.20, 6.22, 6.21, and 6.24). The same structure was observed at La Serrata using magnetotellurics (Fig. 5.23). The CFZ has been active at least since the Late Miocene with an interrupted activity during the Pliocene and Quaternary periods as evidenced by the accumulative degree of deformation observed along the seismo-stratigraphic units infilling the sub-basins (e.g IM-10 profile in Fig. 6.18). The fault zone affects the Quaternary sediments despite being narrower across these than in the basement, as observed systematically in seismic profiles (e.g. HR-MCS profiles in Fig. 6.15). At La Serrata, the apexes of the Late Pleistocene and Holocene fans were gradually separated from the mountain front (units A3.1, A3.2 and A4) (Fig. 4.2) as a result of a decrease in the mountain front uplift at least after 71 ka BP. These observations suggest 1) a decrease in the fault movement, or 2) a change in the fault kinematics, from dip-slip dominated to strike-slip. Two episodes of regional uplift, the first one in the NE part of La Serrata (between ca. 1 Ma BP to 130 ka BP), and the second one in its SW part (later than 71 ka BP) (Fig. 4.17) are suggested.

Evidence of the most recent tectonic activity is also found on land and in the sea. Offshore, high-resolution sub-bottom profiles show fault traces displacing the uppermost reflectors and producing deformation at the seafloor (Figs. 6.11, 6.12 and 6.17). Onshore, the paleo-channel trenched at El Hacho reveals the Holocene activity (section 5.2.6) and constrain the age of a recent (last?) movement of this segment to be younger than AD 775 (which could correspond to the 1522 Almeria earthquake). Younger deposits, such as fluvial terraces, do not completely overlap the fault zone and therefore cannot be used to further constrain the activity of the fault. The fluvial terrace trenched in the Pecho de los Cristos site constrains the last movement of the fault in AD 1450. Therefore, this fault trace (in contrast to the fault trace analysed at El hacho) did not rupture during the 1522 Almería earthquake. Other sub-parallel traces not interacting with recent sediments (and therefore beyond the possibility of a paleoseismic analysis) may account for the 1522 Almería earthquake at the Pecho de los Cristos.

8.1.2. Evidence of block tilting along the CFZ

Offshore, a scissor-type vertical movement of the NW block, first suggested by Gràcia et al. (2006), is confirmed with a relative uplift towards the SW and subsidence to the NE (Fig. 6.24). This is consistent with the multi-fractured block escape model proposed by Martínez-Díaz (1998) (Fig. 2.5) with the relative movement and rotation of the sub-blocks limited by the CFZ, the Alpujarras Fault Zone, and NW-SE normal faults, the last ones controlling the tilting towards the east.

Regarding the onshore observations, the regional distribution of Quaternary deposits along the foot of the NW boundary of La Serrata range suggest at least two episodes of regional uplift, the first one in the NE part of La Serrata (between ca. 1 Ma BP to 130 ka BP), and the second one in its SW part (later than 71 ka BP) (Fig. 4.17). Following the Martínez-Díaz hypothesis, the onshore relative uplifts observed along La Serrata can also be interpreted as a consequence of the eastwards tilting of sub-block model. In this case, two different blocks would be considered: 1) a block to the NE of La Serrata that would give rise to the first observed uplift, and 2) a block to the SW that would give rise to the second observed uplift. A NW-SE normal fault should delimit these two blocks. Such a fault was suggested by Goy and Zazo (1983) with a N140º-160º orientation and poor surface expression. Based on geomorphological observations, these authors propose a normal kinematics for this NW-SE fault uplifting the easternmost area of La Serrata. Further detailed observations of the relative uplift and subsidence along the northwestern block of the CFZ should be carried out systematically in order to localize the main NW-SE faults controlling the block escape model.

8.2. Paleoseismology of the Carboneras Fault Zone

8.2.1. The CFZ as a seismogenic and tsunamigenic fault

Colluvial wedge deposits, observed on the trench walls at El Hacho (Fig. 5.5) and Los Trances (Fig. 5.14), were originated from the degradation of a fault scarp due to sudden surface faulting events. Their sudden occurrence strongly suggests the seismogenic character of the CFZ. This differs from earlier studies that question the earthquake capacity of the CFZ owing to the presence of fault gouges along the NE end of the onshore fault trace (e.g. Rutter et al., 1986; Keller et al., 1995) (Fig. 2.3a). As stated in section 2.4.1, the fault gouges were created during the Miocene extensional stage by the sliding of the metamorphic complexes along low-angle faults (Alonso-Chaves et al., 2004), and later, the CFZ intersected these materials and incorporated them into its fault plane. The presence of these fault gouges along a significant part of the fault surface and at depth has not been demonstrated and the colluvial wedges rules

out an aseismic behaviour, at least along the earthquake segment which includes La Serrata.

As a seismogenic structure, the CFZ is a potential candidate for historical earthquakes in the area, such as the AD 1522 Almería earthquake, as suggested by Reicherter and Hübsher (2006) (Fig. 2.6) who found tsunami deposits in coastal lagoons near Cabo de Gata. The Holocene (post-AD 775) event described at El Hacho (section 5.2.6.4) could correspond to this historical earthquake but its upper age was not constrained and thus, the link of the CFZ with the 1522 earthquake cannot be asserted with certitude. However, the maximum 1.5 m offset observed for the El Hacho event suggests that it corresponds to a large event, lending support to this hypothesis. In any case, other segments of the CFZ, such as the submerged SCF segment may also be considered as potential sources of the AD 1522 earthquake and tsunami (rupturing independently or together with the onshore segment), as well as other offshore structures such as the Adra Ridge Fault or the NW-SE trending faults (Fig. 6.21).

The CFZ can also be considered as a potential source of tsunamis given its seismogenic behaviour and its submerged trace. The CFZ is predominantly a strike-slip fault and therefore may not vertically displace the sea bottom as likely to produce a tsunami. Despite this and because it runs along the considerably dipping slope of the Almería Margin (maximum dipping values of 5.5º) (Fig. 6.2), its horizontal movement could have a significant vertical displacement on the seafloor (e.g. maximum wave elevation at the coast of 0.5 m considering the whole CFZ rupture length; Fig. 8.1).

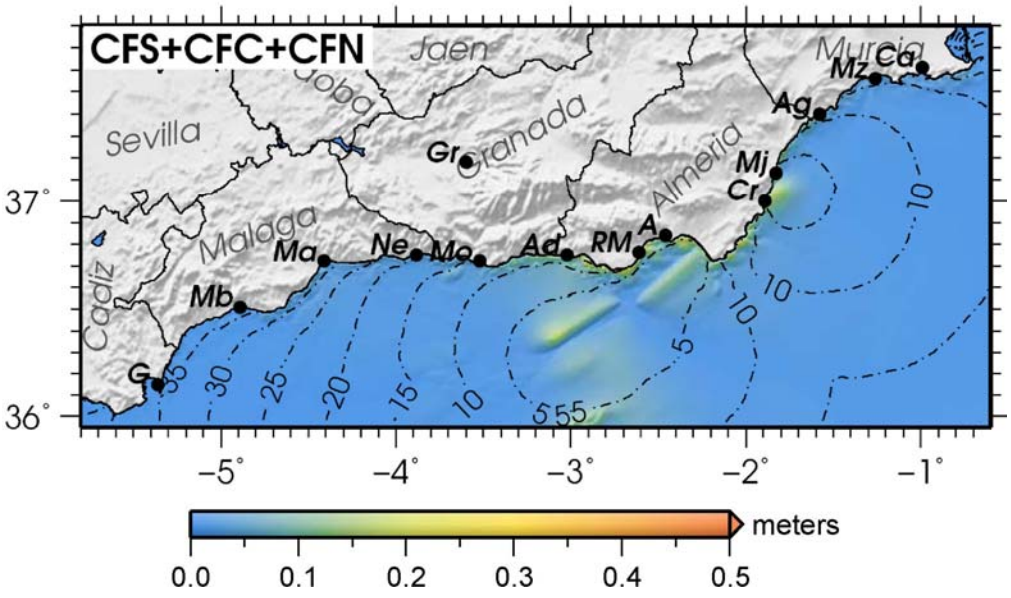

Figure 8.1. Maximum wave elevation map and estimated tsunami travel times in the Alboran Sea considering the entire Carboneras Fault trace. The shading represents the wave elevation value as shown in the colour scale at the bottom. The contours show the tsunami travel time in 5 min steps from the source (Álvarez-Gómez et al., 2011).

Furthermore, the CFZ is not a pure strike-slip structure but it also has a vertical component, which may be increased locally due to the model of eastwards tilting of sub-blocks in the NW part of the CFZ. It should be added that the earthquakes nucleated along the CFZ can also trigger associated submarine landslides (Álvarez-Gómez et al., 2011), as those observed in the bathymetry (e.g. the Chella Slide, Fig. 6.2) which are potential tsunami triggering sources.

8.2.2. Sedimentation rates and climatic stages: Implications for paleo-earthquake reccurrence intervals

The Quaternary deposits identified at La Serrata consist of four successive alluvial fan generations (A1, A2, A3 and A4) and two secondary channel fluvial terraces (Tp and Th). Calcrete crusts and soil development stages were associated with each alluvial unit. In the Almería Margin, the Late Quaternary sedimentary units were described as an alternation of transparent and well stratified TOPAS facies. Quaternary sedimentary units were dated with radiometric analysis (^{14}C, TL, U/Th, ^{10}Be) when possible and these results together with geological and climatic assumptions (relation between sedimentary units characteristics an climatic patterns of sedimentation) allowed us to correlate these sedimentary units with climatic fluctuations defined by the Marine Isotopic Stages (MIS) (Table 8.1). This analysis enhanced the time constraining of each unit (Fig. 8.2) and especially that of the poorly constrained Mid and Late Pleistocene units.

Table 8.1: Synthesis of the onshore and offshore radiometric dating results for each sedimentary (onshore) and seismic (offshore) unit and relationship with the Marine Isotopic stages.

Marine Isotopic stage		Onshore untis (radiometric age)	Offshore units (radiometric age)
MIS 1	(0-14 ka BP)	Th (560-1420yrs BP)	
		Paleo-channel (920-1313 Cal yr BP)	TOPAS unit IV (0-31.1 Cal ka BP)
MIS 2-4	(14-71 ka BP)	A3.1 (20.6-71.6 ka BP)	
			TOPAS unit III
MIS 5	(71-130 ka BP)	Tp (59.5-111.5 ka BP)	TOPAS unit II
MIS 6	(130-191 ka BP)	A2 (last pulse) (>120 ka BP)	TOPAS unit I
MIS 12-6	(191-478 ka BP)	A2	
Early/Mid Pleistocene		A1 (214 ka to c. 1 Ma BP)	

The benthic δ^{18}O global stack curve defined by Lisiecki & Raymo (2005) is used to correlate the sediment units with the MIS stages (Fig. 8.2). The MIS boundaries are defined midway between glacial and an interglacial stages by the difference between the maximum δ^{18}O value of the preceding glacial and the minimum of the following interglacial. The transition from an interglacial to a glacial stage is also established and used to constrain the age of the sedimentary unit stages. This study focused on the following MIS boundaries: MIS1/2 boundary of 14 ka BP, MIS4/5 boundary of 71 ka, MIS 5/6 boundary of 130 ka, MIS 6/7 boundary of 191 ka. It should be noted that

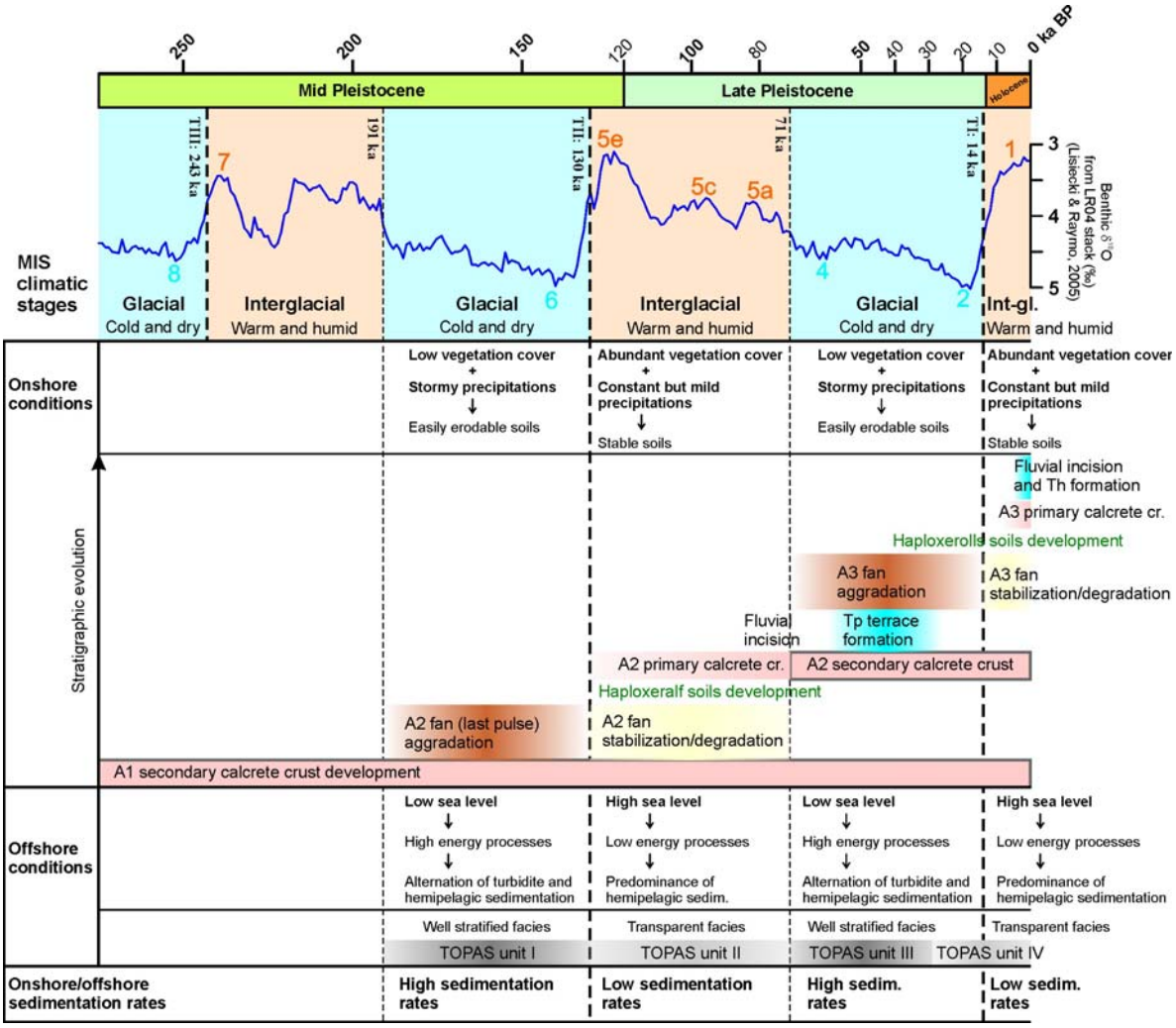

Figure 8.2. Correlation between marine isotopic climatic stages (MIS) and onshore-offshore sedimentation units along the CFZ.

the ages of these boundaries were established as average midpoints from the global curve, and do not necessarily correspond to the precise timing when a sedimentation pattern changes in a given region, possibly leading to several thousands of years of error. This is evidenced in the transparent pattern of TOPAS unit IV, which should be theoretically associated with the last interglacial stage, whose base has been dated as 14 ka BP. ^{14}C analysis of a sample at the base of the unit yielded an age of 31.1 Cal ka BP (Fig. 7.9), suggesting that the end of MIS 2-4 stage was characterized by a low energy process pattern in the study area. Climatic/geological assumptions were used in the absence of direct dating and an approximation to the age of the sedimentary units was obtained by correlating them with the MIS boundary ages. If this had not been achieved, it would have been necessary to date these units by extrapolating a fixed sedimentation rate (in the case of marine sediments) or leave them undated. Correlating sedimentary units with MIS stages was essential to constrain the ages of some of the Middle and Upper Pleistocene units that was not always achieved by numerical dating methods.

Dating these old deposits was the key to obtaining paleoseismic results because the CFZ is a slow moving fault ant therefore requires observation of long periods of time.

The sedimentation rate is higher during cold stages than during warm stages as deduced from the analysis of sedimentation patterns. A glacial stage is characterized by onshore fan aggradation and offshore alternation of turbidites and hemipelagic sedimentation. In contrast, an interglacial stage is characterized by onshore fan stabilization and degradation, and a predominantly hemipelagic sedimentation offshore (e.g. Harvey, 1990; García et al., 2006). A fast sedimentation rate yields a better resolution to characterize paleo-earthquakes. A low sedimentation rate yields little resolution. Finally, a discontinuous sedimentation may imply an incomplete paleo-earthquake record. This has important implications for paleoseismic analysis since too little resolution or intermittent sedimentation tends to overlook paleo-events, leading to an overestimation of the mean recurrence period and hence to an underestimation of the seismic activity of the region. Mean recurrence periods are usually understood as maximum values since some earthquakes may not have been preserved in the geological record, but in areas where a big dichotomy between climatic periods prevails, the probability of overestimating a recurrence period (especially for slow faults) from geological observations is strengthened.

8.2.3. Slip-rates

The slip-rate of a fault represents the average of the total slip along a fault and over a certain period of time. Slip-rates are used to estimate the level of activity of a fault and thus the hazard that this may represent to an area. Moreover, the analysis of slip-rates can also provide information about changes in the fault activity along its history. In the CFZ, slip-rates were calculated by identifying vertically and horizontally offsets. The results are summarized in table 8.2.

Slip-rate values are calculated using offset dated landforms. The offset of a feature may have occurred long after its formation and therefore long after the numerical age. Consequently, the maximum values of slip-rate normally lack of sense. This is especially true when looking at long-term slip-rates such as slip rates since the Late Pliocene obtained from the HR-MCS profiles (Table 8.2). However, when a continuous fault activity through the whole Quaternary is demonstrated, this uncertainty is minimized. For instance, when analyzing TOPAS profiles, this error is considered to be insignificant compared to the concept that hemipelagic sediments may drape the uppermost layers, and thus the apparent vertical offset measured must be considered as a maximum value resulting in a maximum dip-slip rate. In the case of the offset paleo-channel at El Hacho, the approach is different as single events can be distinguished. At this site, two events are interpreted and the last one may correspond to the last event, i.e. a seismic cycle has not yet been accomplished. Therefore, the average strike-slip rate is

a maximum value. A thorough understanding of the landform is essential for a good interpretation of the result.

Table 8.2: Synthesis of the onshore and offshore slip-rates calculated along the Carboneras Fault Zone. NWSB: Northwest Serrata Boundary.

	Geomorphological evidence	Observed at	Min. value	Max. value
Strike-slip rates	Offset paleo-channel	El Hacho site (NWSB)	0.05 mm/yr (since 32.1 ka BP)	1.3 mm/yr (since 1175 Cal yr BP)
	Deflected drainage	El Hacho and Pecho de los Cristos sites (NWSB)	1.1 mm/yr (since 130 ka BP)	
	Deflected gullies	Dalías TVS (offshore NCF segment)	1.3 mm/yr (since 1.8 Ma BP) 1.3 mm/yr (since 3.6 Ma BP)	
Dip-slip rates	Colluvial wedges	El Hacho site (NWSB)	0.02 mm/yr (since 130 ka BP)	
	A2 calcrete crust	Pressure ridge (NWSB)	0.15 mm/yr (since 130 ka BP)	
	A1 alluvial fan	Cerro Blanco site (NWSB)	0.05 mm/yr (since 1 Ma BP)	
	Offset TOPAS reflectors	Offshore NCF-3 sub-segment		0.1-0.3 mm/yr (since 130-191 ka BP)
	Offset HR-MCS reflectors	Offshore NCF-3 and SCF-6 sub-segments	0.01-0.05 mm/yr (since 3.6 Ma BP) 0.01-0.05 mm/yr (since 2.6 Ma BP) 0.03-0.05 mm/yr (since 1.8 Ma BP)	

Results on the strike-slip component of the slip-rates are comparable (Table 8.2). The minimum value obtained at El Hacho based on the offset paleo-channel (0.05 mm/yr since 32.1 ka BP) is considerably undervalued as suggested in section 5.2.6.3 because of the poorly constrained lower age for the 1.5 m maximum slip. The rest of the minimum strike-slip rate values are consistent (1.1-1.3 mm/yr) despite having been calculated for different periods. A similar value is also obtained as a maximum strike-slip rate based on the paleo-channel offset since 1175 Cal yr BP. Three interpretations account for the Holocene strike-slip rate: a) the Holocene strike-slip rate is lower than the Pliocene and Pleistocene rates, b) the Holocene strike-slip rate is close to its maximum (1.3 mm/yr) and therefore to the long period strike slip rate, or c) the strike-slip rate is 1.1-1.3 mm/yr at the fault trace bounding La Serrata to the NW, but, an additional slip is absorbed by the SE trace which was not considered in this study (although it probably belongs to the same seismogenic structure at depth according to the 2D magnetotelluric model). In the last case, the 1.1-1.3 mm/yr corresponds to a minimum value and the total strike-slip rate is larger than 1.3 mm/yr as suggested by the offshore gullies. In agreement with this last option, preliminary results from GPS analyses suggest a 1.5±0.7 mm/yr of left-lateral strike-slip motion at the CFZ with a

minor compressive component of 1.0±0.7 mm/yr (Fig. 2.13) (Khazaradze et al., 2010). This result rules out option a (a decrease in the strike-slip rate during the Holocene). Therefore, a minimum Quaternary strike-slip rate of 1.3 mm/yr is proposed. However, as all the left-lateral offset values were measured along the Northern Carboneras Fault segment (onshore and offshore), the suggested minimum strike-slip rate refers only to this segment.

Dip-slip rates (Table 8.2) show a wide range of results depending on the area and time span. This is consistent with a) what is expected for a strike-slip structure, such as the CFZ, laterally displacing an irregular topography, and with b) what is expected according to the tilting sub-block model proposed for the NW block of the CFZ. It can be stated that the dip-slip rates are one to two orders of magnitude lower than strike-slip rates, which supports the view that the CFZ is a predominantly left-lateral structure with a minor vertical component.

8.2.4. Estimations of the mean recurrence period

A minimum of 7 events are evidenced since 191 ka BP along the NW boundary of La Serrata, the last event being younger than AD 775. A mean recurrence period of 27.3 ka (Fig. 5.24) is thus inferred for the last 191 ka. However, the age of the older events (L1, L2, E1 and E2 in Figs. 5.15 and 5.8) is very poorly constrained and this is probably enlarging the calculated mean recurrence interval. Taking into account only the last three events at El Hacho (E3, Ea, Eb in Fig. 5.12) which occurred since 41.5 ka BP, the mean recurrence period decreases to 13.8 ka, a value similar to the mean recurrence obtained in the northern Alhama de Murcia Fault (Martínez-Díaz et al., 2001; Masana et al., 2004). Furthermore, geomorphological observations related to the last two events (Ea and Eb) suggest a shorter interval of a few thousand years between two successive earthquake events, which could be interpreted either as a shorter mean recurrence period for the CFZ or as a clustering.

It was not possible to obtain offshore values of the mean recurrence period of the CFZ as single earthquake events could not be identified in the acoustic and seismic data. Near seafloor high-resolution systems, such as the ones included in Remotely Operated Vehicles (ROV) for visual inspection, micro-bathymetry and ultra-high resolution seismic systems are required to identify earthquake events under water. Such a study has successfully been carried out along the offshore segments of the North Anatolian Fault under the Marmara Sea, where seafloor surface ruptures of past historical earthquakes have been identified using the ROV Victor 6000 (e.g. Armijo et al., 2005). Nevertheless, based on pre-existing dated of sediment cores from the Almería Canyon (Bozzano et al., 2009), a speculative attempt to turbidite paleoseismology analysis yield results that are surprisingly similar to those obtained at El Hacho. A maximum elapsed time since the last turbidite event (i.e. earthquake if interpreted as seismically triggered)

of 1.3 ka is inferred. If the previous event is taken into account, a minimum elapsed time between turdidites of about 13 ka is obtained.

In summary, the 13.8 ka mean recurrence period obtained at El Hacho is close to the 14 ka value obtained at the Alhama de Murcia Fault (Martínez-Díaz et al., 2001; Masana et al., 2004) and the 13 ka result tentatively obtained from the turbidite deposits offshore. However, on the assumption of a characteristic fault behaviour, it is also possible to estimate the recurrence interval of a fault by dividing the displacement during a single event by the slip-rate (Wallace, 1970). Assuming a minimum strike-slip rate of 1.3 mm/yr (based on the deflected drainage along the NW Serrata boundary) and a maximum slip per event of 1.5 m (based on the maximum paleo-channel offset at El Hacho), a maximum return period of 1150 years is obtained. This result is consistent with the inferred return period between the two last events at El Hacho (events Ea and Eb) estimated to be in the order of a few thousands of years. A global analysis of the results obtained along the fault trace suggest, therefore, that the recurrence is one order of magnitude lower (about 1.1 ka) than that obtained from trenching surveys (about 13.8 ka). This is line with the assumption that low sedimentation rate periods implies low resolution which in turns contributes to an overestimation of the recurrence period calculated from an incomplete paleo-earthquake record.

8.3. Tectonic architecture of the CFZ and its implications for earthquake segmentation

8.3.1. Sub-surface tectonic architecture of the CFZ

A dense net of high-resolution seismic profiles (Fig. 6.11-6.15 and6.17-6.20) showing a large variety of structures allowed the offshore observation of the sub-surface tectonic architecture of the CFZ. The NCF segment, trending N047º, starts with a flower structure on the shelf, evolves to parallel fault traces bounding a pressure ridge, and finally to a narrow vertical fault zone. The northern part of the SCF segment, shows two successive pressure ridges trending N059º and keeps the same orientation along a narrow vertical fault zone. To the south, the SCF segment changes its orientation to N050º maintaining the narrow fault zone structure. The 2D magnetotelluric model obtained across La Serrata (Fig. 5.23) suggests a flower structure controlling the range in this onshore area.

The two methods, MCS and MT, reached only the upper 1-2 km below the surface. Therefore, the fault traces are not clearly observed merging at depth into a single seismogenic structure. To observe the fault structure below the 2 km depth, higher penetration systems, such as a larger volume source (> 3000 c.i.) and a longer streamer (> 3 km long) MCS and a longer period broad-band magnetotellurics, should be employed. However, a deeper penetration implies a lower resolution, and thus two traces separated by 2 km would probably not be distinguished. Despite this, a

convergence at depth is the most probable structure given the short separation between faults of a structure that is considered to cross all the fragile crust keeping a sub-vertical pattern (Pedrera et al., 2010).

8.3.2. The southern and northern ends of the CFZ: strain transfer to other nearby structures

The nature of the southern end of the CFZ was widely discussed in section 6.5.4. The deformation of the fault decreases towards the south and is gradually transferred to the Adra Ridge Fault and eventually to the Yussuf Fault, first through a shear fault zone, and then through the pervasive faulting zone of the Yussuf Fault horsetail splay (Fig. 8.3).

To the north, the CFZ ends in a triple fault junction with the E-W trending Corredor de las Alpujarras Fault Zone (CAFZ), and the NNE-SSW trending Palomares Fault (PF) (Fig. 8.3). This triple fault junction is formed by a wide deformation zone with small fault traces of different orientations, especially in the convergence zone between the CAFZ and the CFZ. The offshore extension of the CFZ to the NE has not been identified in the shelf maps available (ESPACE project, IEO), and there is no bathymetric evidence of any fault lineation further to the NE in contrast to what is observed at its SW offshore extension in the Almería Margin. This suggests that the northeastern tip of the CFZ ends abruptly at the triple fault junction and does not continue offshore. Thus, the deformation in the northern end of the CFZ is apparently transferred to the PF and CAFZ structures.

8.3.3. Segmentation of the CFZ

The absence of well-recorded historical or instrumental seismicity along the CFZ prevents us from establishing a segmentation based on the seismicity along the fault. A segmentation is proposed here based on geomorphological and structural observations to assess the seismic hazard and to better understand fault mechanics. Two scales of structural segmentation were proposed. First-order segments were defined on the basis of geomorphological observations (i.e. changes in the fault trace orientation). Second-order segments were defined offshore on the basis of fault structure variations in the upper kilometres below the seafloor, and onshore on the basis of geomorphological variations. This segmentation analysis will be used to extrapolate the paleoseismic results at La Serrata to the entire fault segment.

Offshore first-order segments correspond to the N047º trending North Carboneras Fault (NCF) segment and the N059º/050º trending South Carboneras Fault (SCF) segment. This change in the fault trace orientation is thought to be caused by the interaction of the fault zone with the shear zone in the SE part of the SCF (section 6.5.4) represented on surface by NW-SE trending folds (Fig. 8.3).

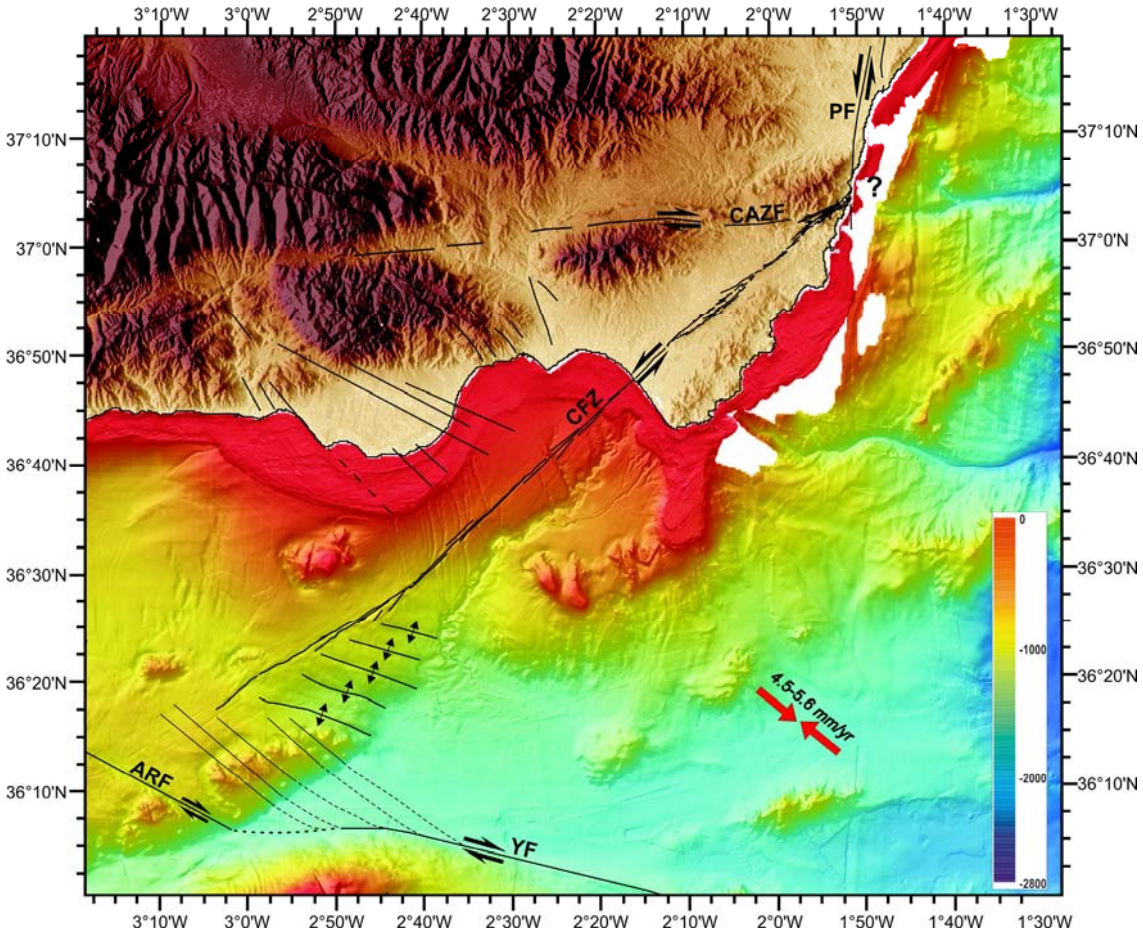

Figure 8.3. Topographic map of the SE part of the Almería province and bathymetric map of the Almería Margin. The main structures are located. Opposite pointing red arrows show the direction of convergence between the Eurasian and African plates from NUVEL1 model (Argus et al., 1989; DeMets et al., 1990). PF: Palomares Fault; CAFZ: Corredor de las Alpujarras Fault Zone; CFZ: Carboneras Fault Zone; ARF: Adra Ridge Fault; YF: Yussuf Fault.

Following the fault orientation criterion, the entire emerged portion of the CFZ is considered to belong to the NCF segment, since it maintains an average N050º, very close to the N047º defined offshore (Fig. 8.4). Onshore variations in the orientation can also be observed. In the central part of the emerged CFZ, a 13 km long trace trending N060º (Fig. 8.4) is observed. This is considered a splay diverging from the main fault trace, which apparently continues with a dominant N050º orientation. To the north of the N060º splay, the fault zone becomes wider and complicated, with a larger number of short fault traces and a large variety of trace orientations. As, suggested above, this is due to the convergence between the CAFZ and the CFZ (Fig. 8.4). The general trending of the fault zone, however, follows the dominant N050º orientation.

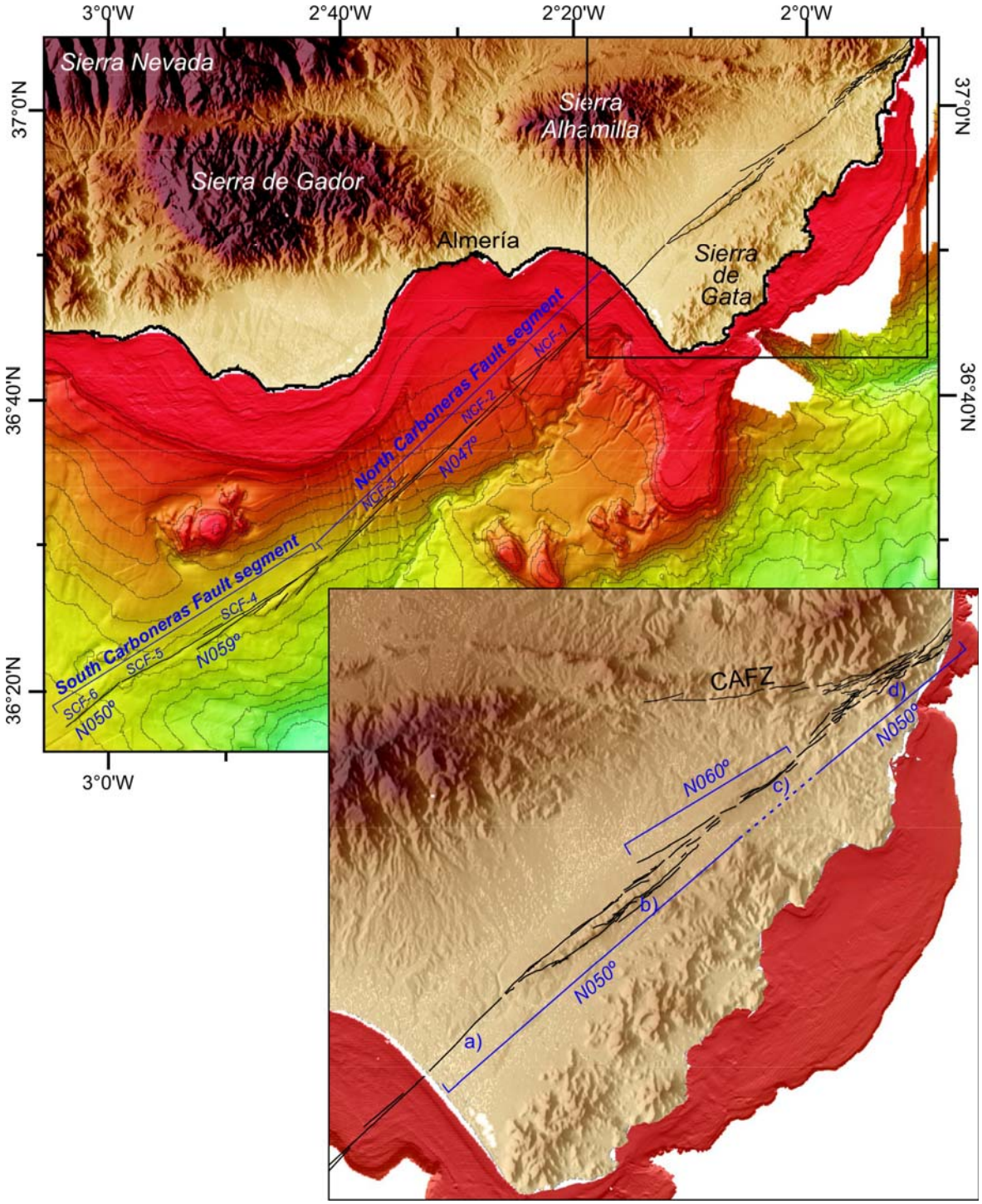

Figure 8.4. Topographic map of the SE part of the province of Almería and bathymetric map of the Almería Margin with location of the different segments and sub-segments proposed for the CFZ. Offshore contour interval is 100 m. CAF: Corredor de las Alpujarras Fault Zone.

In summary, two main first order segments are proposed for the CFZ according to a considerable change in the fault trace orientation: a northern one trending N047º/050º which includes the emerged portion of the fault and a southern one trending

N050º/059º. The average parameters of the onshore-offshore North Carboneras Fault (NCF) and of the Southern Carboneras Fault (SCF) segments are listed in Table 8.3.

Table 8.3: Parameters characterizing the two first-order segments defined for the CFZ

	NCF	SCF
NE tip coordinates	37º05'06''N - 1º50'57''W	36º29'10''N - 2º41'31''W
SW tip coordinates	36º29'10''N - 2º41'31''W	36º17'41''N - 3º03'39''W
Length	100 km	39 km
Average orientation	N048.1º	N057.2º

Offshore second-order sub-segments were differentiated according to structural variations identified in the seismic profiles. A total of 6 structural sub-segments were defined (see Table 6.2 for parameters of each sub-segment): 3 for the submerged part of the NCF segment (NCF-1, NCF-2 and NCF-3) and 3 for the SCF segment (SCF-4, SCF-5 and SCF-6) (Fig. 8.4). These are characterized, from north to south by: NCF-1) a positive flower structure, NCF-2) a vertical fault zone forming a pressure ridge, NCF-3) a N047º trending narrow vertical fault zone, SCF-4) a fault zone with prominent pressure ridges, SCF-5) a N059º trending narrow vertical fault zone, and SCF-6) a N050º trending narrow vertical fault zone. Onshore, little data is available on the sub-surface (only at La Serrata where magnetotellurics showed the upper 2 km below the surface). An attempt to define second order sub-segments is, however, presented according to changes in the surface expression of the fault trace. From south to north these onshore segments are (Fig. 8.4 and table 8.4): a) a single trace with poor surface expression, b) two parallel fault traces at La Serrata (inferred to be a flower structure at depth according to magnetotellurics), c) a narrower fault zone, and d) a complex wide fault zone. These are coincident with the segments proposed by García-Mayordomo (2005) and named: Rambla Morales (a), La Serrata (b), El Argamasón (c) and Carboneras (d). However, more information about the sub-surface structure is required to accurately define these sub-segments.

The northern offshore sub-segment (NCF-1) was described as a 4-5 km wide deformation zone formed by a flower structure at depth (see profile IM-18 in figure 6.13). However, the most active faults are concentrated in a 1-1.5 km wide fault zone (see profile EVE-1 in Fig 6.13) with poor surface expression, especially on the shelf where only small seafloor deformation is observed. This poor surface expression continues onshore to the north, along the NCF-a sub-segment, which has no depth geophysical imaging. Further north, at La Serrata, sub-segment NCF-b is interpreted as a flower structure by the 2D magnetotelluric model (Fig. 5.23), here with a strong surface expression. Then, the boundary between sub-segments NCF-1 and NCF-a is placed at the shoreline, for practical reasons (differences in the availability of

Table 8.4: Parameters described for each structural sub-segment for the entire CFZ

First order segment	Second order segment	SW tip coordinates (longitude, latitude)	Orientation (of the main fault trace)	Average	Length (km)	
NCF	NCF-d	1º 56' 40'' W , 37º 01' 05'' N	N055.0º	N050º	11	48
	NCF-c	2º 01' 03'' W , 36º 57' 52'' N	N050.0º		10	
	NCF-b	2º 12' 07'' W , 36º 50' 43'' N	N051.0º		20	
	NCF-a	2º 15' 45'' W , 36º 47' 50'' N	N044.6º		7.5	
	NCF-1	2º 25' 20'' W , 36º 40' 45'' N	N047.3º	N047º	19	51
	NCF-2	2º 28' 35'' W , 36º 38' 12'' N	N045.4º		7	
	NCF-3	2º 41' 19'' W , 36º 29' 17'' N	N046.8º		25	
SCF	SCF-4	2º 52' 51'' W , 36º 23' 14'' N	N057.7º	N059º	20	39
	SCF-5	2º 58' 43'' W , 36º 20' 37'' N	N062.0º		10	
	SCF-6	3º 03' 34'' W , 36º 17' 32'' N	N050.3º	N050º	9	

information and methodological approach) and lacks structural sense. Thus, it could be reasonable to considered that the offshore NCF-1 sub-segment does not stop at the shoreline but continues towards the north through the NCF-a and probably the NCF-b sub-segments, forming a flower structure at depth. The locally poor surface expression of NCF-1 and NCF-a could be attributed to a higher erosion near the coast. However, further sub-surface imaging is needed to confirm this.

8.3.4. Maximum moment magnitude estimations

To obtain maximum magnitudes for paleo-earthquakes, the surface rupture length and the maximum displacement are the most commonly used parameters (e.g. Bonilla et al., 1984; Wells and Coppersmith, 1994). The inferred rupture length and slip for a given fault is compared to a worldwide catalogue compiling rupture lengths and slips of historical and instrumental earthquakes (i.e. with known magnitude), thereby allowing us to estimate a probable paleoearthquake magnitude.

The empirical relationships of Wells and Coppersmith (1994) provide an estimation of the maximum moment magnitude (Mw) related to the maximum surface rupture length (SRL) based on the following equation:

Mw = a + b * log (SRL) where a = 5.16 +/-0.13 and b = 1.12 +/-0.08 are the coefficients obtained for strike-slip faults. For this equation the standard deviation is s=0.28 and the correlation coefficient is r = 0.91.

For slow-to-moderate faults, such as the CFZ, earthquake segment boundaries, defined at seismogenic depths (Schwartz and Sibson, 1989), are barely observed and geometric segment lengths are used to evaluate the maximum surface rupture lengths. The structural changes described along segments and sub-segments for the CFZ do not

necessarily represent the fracture arrest during an earthquake, but they could pose a problem for the transmission of the rupture. The entire 140 km long onshore-offshore fault trace could be considered too long for rupturing during one single event, although this possibility cannot be ruled out. The length of the defined segments and sub-segments are used to calculate their maximum magnitudes using the Wells and Coppersmith (1994) SRL/Mw empirical relationship defined above. Results are listed in table 8.5.

Table 8.5: Maximum moment magnitude (Mw) estimated for each segment and sub-segment of the CFZ according to its maximum surface rupture length.

1st order segment	Length (km)	Maximum Mw	1st to 2nd order segment	Length (km)	Maximum Mw	2nd order segment	Length (km)	Maximum Mw
NCF	100	7.4 +/- 0.3	N050º NCF	48	7.0 +/- 0.3	NCF-d	11	6.3 +/- 0.2
						NCF-c	10	6.3 +/-0.3
						NCF-b	20	6.6 +/-0.3
						NCF-a	7.5	6.1 +/- 0.2
			N047º NCF	51	7.1 +/- 0.3	NCF-1	19	6.5 +/-0.3
						NCF-2	7	6.1 +/-0.1
						NCF-3	25	6.7 +/-0.3
SCF	39	7.0 +/- 0.3	N059º SCF	30	6.8 +/- 0.3	SCF-4	20	6.6 +/-0.3
						SCF-5	10	6.3 +/-0.3
			N050º SCF	9	6.2 +/- 0.3	SCF-6	9	6.2 +/- 0.3

Crustal spatial discontinuities, such as changes in the fault trace orientation or significant fault step-overs, may control the seismogenic segments rather than changes in the superficial architecture (i.e. uppermost kilometres below the seafloor). Thus the maximum magnitudes calculated for the 2nd order segments (sub-segments), ranging between Mw 6.1 +/-0.2 and Mw 6.7 +/-0.3 (Table 8.5), have little paleoseismic significance. When considering changes in the fault trace orientation (first order segments), maximum magnitudes increase up to Mw 7.4 +/-0.3 for the whole NCF segment, and Mw 7.0 +/-0.3 for the whole SCF segment (Table 8.5). Taking into account smaller orientation changes along the SCF segments, maximum magnitudes range between Mw 6.2 +/-0.3 for the N050ºtrending SCF sub-segment and Mw 7.1 +/-0.3 for the N047º NCF sub-segment (named as 1st to 2nd order segment in Table 8.5). The change of orientation along the NCF segment is actually very small, and the boundary at the shoreline has little meaning, and thus, the resulting maximum magnitudes have poor paleoseismic significance. Finally, there is no significant reason to rule out a rupture all along the CFZ during a large earthquake. In this worst case scenario, the maximum magnitude for the entire CFZ is calculated. According to the 140 km long fault trace, a maximum Mw 7.6 +/-0.3 is obtained.

Another way to estimate the maximum magnitudes was achieved by the maximum slip per event calculated from the paleo-channel offset and by the thickness

of the colluvial wedges at El Hacho (sections 5.2.5, 5.2.6 and 5.2.8). The maximum magnitudes were obtained using the relationships proposed by Wells and Coppersmith (1994) which relate the estimated moment magnitude and the maximum displacement. A maximum Mw of 6.9-7.0 was obtained using the paleo-channel offset and a Mw of 6.4->6.9 was obtained using the colluvial wedge thickness. The former result was preferred since the fault is dominantly strike-slip and given the uncertainties of vertical slips observed along such a structure (see section 5.2.5.3). The maximum Mw 6.9-7.0 obtained refers to the NCF segment, along which El Hacho site is located. This value is lower than the one calculated for the entire NCF segment if the maximum surface rupture length is considered. Several hypotheses are suggested: 1) the earthquake that ruptured the paleo-channel was not the maximum earthquake that the fault segment is capable to produce; 2) the NCF segment hosts several shorter segments and only part of the first order segment ruptured, and 3) the strain release was distributed along several fault traces of the fault zone during this earthquake, and thus the results from El Hacho are minimum values.

8.4. The Carboneras Fault Zone in its geodynamic context: the Eastern Betic Shear Zone and the Trans Alboran Shear Zone

The Eurasian and African plates converge at a rate of 4.5-5.6 mm/yr in a NW-SE direction according to the NUVEL1 model (Argus et al., 1989; DeMets et al., 1990) (Fig. 8.3). Considering that the CFZ is a dominantly strike-slip structure with a minimum strike-slip rate of 1.3 mm/yr, as proposed in this study, it absorbs at least a 23.2% of the total convergence. Other structures from the plate boundary, such as faults of the Eastern Betic Shear Zone (EBSZ) to the north, faults from the Trans Alboran Shear Zone (TASZ) to the SW, the Yussuf Fault to the SE or other faults in the north of the African continent, may be absorbing the rest of the deformation. The Carboneras Fault together with the Alhama de Murcia Fault and the Yussuf Fault are the longest structures along the plate boundary and may be absorbing an important part of the deformation. However, other smaller structures should not be underestimated.

Paleoseismic studies were recently carried out along some of these structures, such as the Alhama de Murcia Fault (Martínez-Díaz et al., 2001; Masana et al., 2004), where the recent 2011 Lorca earthquake produced loss of life and considerable damage to infrastructure. However, other structures from the plate boundary are poorly known from a paleoseismic point o view, such as the faults in the north African Margin (e.g. Al Idrissi Fault near Al-Hoceima), which should be considered as additional sources in the seismic hazard assessment models.

8.5. Perspectives for future research along the Carboneras Fault Zone

Onshore and offshore fields are usually not merged, forcing a structure limit at the shoreline. This lack of land-to-sea connection can lead to a dangerous underestimation of the fault parameters (geometry, number of segments, etc.) with serious implications for seismic hazard modelling. Despite its limitations (i.e. the fault not being directly accessible for observing, sampling and measuring at its intersection with the Earth surface), the young marine paleoseismology discipline has clear advantages (i.e. good spatial coverage, continuous sedimentation throughout a long temporal span, minimized erosion, and very limited human modification) (Pantosti and Gràcia, 2010). Combining onshore and offshore analyses along the same structure allows us to make full use of each environment, direct fault observations onshore and continuous sedimentation and well preserved geomorphology offshore.

In this thesis, an integrated onshore-offshore analysis is presented and demonstrates the success of integrating onshore-offshore analysis. According to the good results obtained in this study, further paleoseismic analysis should be considered in order to better constrain the paleoseismic parameters of the CFZ and to better assess its implications for the seismic hazard of the region.

Onshore, paleoseismic analysis should continue a) to extend the detailed geomorphological mapping to the NE and to the SW of La Serrata, b) to undertake additional 2D and 3D trenching surveys along the fault trace, c) to enhance the age constraints by additional dating analysis using traditional and new techniques, and d) to acquire and analyze detailed DTM based on the Laser Imaging Detection and Ranging (LIDAR) system. Some specific targets are proposed:

1) To reduce uncertainty in dating Quaternary sediments in order to better constrain the ages of the events identified and the slip-rates calculated. To this end, the use of different techniques, such as regional soil chronosequence or Optical Stimulated Luminiscence (OSL) are proposed.

2) To extend the paleoseismic analysis with 2D and 3D trenching at the SE boundary of La Serrata, where suitable paleoseismic sites were described, such as the uplifted A2 apex (Fig. 4.11) close to El Hornillo (section 4.4.1).

3) To extend the paleoseismic analysis to the NCF-c sub-segment where the fault trace is narrow and where some recent deposits locally cover it. Recent sediments are absent in the northern NCF-d sub-segment and the convergence with the E-W trending CAFZ (Fig. 8.3) makes the separation of the deformation attributed to each structure difficult. As regards the NCF-a sub-segment, the area is densely affected by human construction (greenhouses) and detailed paleoseismic studies will be difficult to carry out.

4) To explore in detail and measure the offsets of morphological features on high-resolution DEM based on LIDAR data in order to obtain an enhanced mapping of the active fault traces.

Offshore, near-bottom, higher resolution systems, such as Remotely Operated Vehicles (ROV) for visual inspection, *in situ* sampling, micro-bathymetric surveys or ultra-high resolution sub-bottom profiling would enable us to attain the accuracy demanded for marine paleoseismic studies (i.e. identifying surface ruptures or detecting single earthquake events in seismic profiles) (e.g. Armijo et al., 2005; Barnes and Pondard, 2010). Specific targets are proposed:

1) To use higher resolution systems, such as ultra-high sub-bottom profiling, in areas where the fault trace was inferred to reach up to the surface in order to identify young earthquake ruptures and to recognize single event horizons. This, together with *in situ* sampling, would allow us to date the individual event horizons and to obtain accurate slip-rates.

2) To acquire micro-bathymetry mapping of sites where young features may be offset by the fault. For instance, a higher-resolution bathymetry over the faulted landslide at the NCF-3 sub-segment (Fig. 7.13) would help to observe lateral displacements of this feature.

3) To extend the use of Sparker-like systems along the fault zone in order to obtain a better imaging of features. For example, a higher resolution of the deflected gullies would be helpful to better constrain the timing when these structures started to be active and thus to better constrain the strike-slip rate inferred from their offset.

4) To use long coring systems in the Almería Margin in order to perform radiometric dating of longer sediment record and thus more accurately constrain the ages of the seismic units (specifically the TOPAS units). This would ensure more reliable ages to calculate slip-rates.

Chapter 9: Conclusions

The Carboneras Fault Zone (CFZ) has been active at least since the Late Miocene and has been continuously active during the Pliocene and Quaternary. During Quaternary times, the CFZ concentrated its activity in a narrower fault zone than in previous periods.

The seismogenic character of the CFZ is evidenced by the occurrence of the colluvial wedges observed on the trench walls. The CFZ is, therefore, a plausible candidate for having produced historical earthquakes and tsunamis in the study area, the latest one being triggered either by surface ruptures or associated landslides in the Almería Margin slope.

The Late Quaternary fault activity is evidenced by onshore and offshore faulted deposits. The most recent paleo-earthquake detected, inferred from a faulted paleo-channel, is younger than AD 775. This correlates in time with the historical AD 1522 Almería earthquake and tsunami. However, other segments of the CFZ could also be considered as potential sources for this historical event such as the submerged SCF segment, the Adra Ridge Fault or the NW-SE trending faults to the northwest of the CFZ.

Quaternary sediments were dated with radiometric analysis (^{14}C, TL, U/Th, ^{10}Be) onshore and offshore. Dates together with geological and climatic assumptions allowed the correlation of the sedimentary units with climatic fluctuations defined by the Marine Isotopic Stages (MIS). Onshore, four alluvial fan generations (A1, A2, A3 and A4) and two secondary channel fluvial terraces (Tp and Th) are the main Quaternary deposits identified. From old to young, A1 alluvial fans are most likely of Early Pleistocene age although radiometric analysis yields a wide age range between 214 ka BP to *ca.* 1 Ma BP. A2 alluvial fans are interpreted as Mid Pleistocene deposits and are associated with the cold stages of MIS 12-6 (478-130 ka BP), the last pulse of this unit being related to MIS 6 (190-130 ka BP). Tp fluvial terraces were formed during the warm stage MIS 5 (130-71 ka BP) and yield ages constrained between 111.5 ka BP and 59.5 ka BP. A3 alluvial fans were formed during MIS 4-2, and A3.1 yields an age between 71.6 ka BP and 20.6 ka BP. The young faulted paleo-channel has an age ranging between 1313 Cal yr BP and 920 Cal yr BP. Th fluvial terraces are interpreted as having been formed during MIS 1 and different late Holocene ages range between 1420 Cal yrs BP and 560 Cal yrs BP. Crusts formed on top of A1 and A2 alluvial fans were described and divided into primary and secondary calcrete. Primary calcretes were formed during the first stabilization phase after the aggradation period of the fans, i.e.

A2 primary calcretes were formed during the MIS 5 stage (130-71 ka BP). Secondary calcretes were formed on top of primary calcretes during successive stages, and only where younger deposits were superposed, i.e. A2 secondary calcretes were formed after the end of MIS 5 stage. Offshore, an alternation of well-stratified and transparent facies enabled us to identify four Late Quaternary seismic units (from old to young, units I, II, III, and IV). Well-stratified unit I is estimated to have been deposited during the cold MIS 6, its base being at 191 ka BP. Semi-transparent unit II is estimated to have been deposited during the warm MIS 5, its base being at 130 ka BP. Well-stratified unit III is estimated to have been deposited during cold stages MIS 2-4, its base being at 71 ka BP. The base of the uppermost unit IV was dated by ^{14}C as 31.1 Cal ka BP.

The CFZ is usually vertical despite showing a variety of structures in the first kilometres below the surface, represented by flower structures, pressure ridges and narrow vertical fault zones. The deformation at the southern end of the CFZ decreases towards the south and is gradually transferred to the Adra Ridge Fault and eventually to the Yussuf Fault, first through a fault shear zone, and then through the pervasive faulting zone at the Yussuf Fault horsetail splay. To the north, the CFZ ends abruptly in a triple fault junction with the Corredor de las Alpujarras Fault Zone and the Palomares Fault, and the deformation seems to be transferred to these structures. However, further detailed bathymetric analysis on this offshore NE continuation of the fault should be carried out to confirm this hypothesis.

Onshore, the regional distribution of Quaternary deposits suggest at least two episodes of regional uplift, the first one in the NE part of La Serrata (between ca. 1 Ma BP to 130 ka BP), and the second one in its SW part (later than 71 ka BP). Offshore, a scissor-type vertical movement of the NW block, was confirmed with a relative uplift towards the SW and subsidence to the NE. These observations are consistent with the multi-fractured block escape model proposed by Martínez-Díaz (1998) with the relative movement and rotation of the sub-blocks limited by the CFZ, the Alpujarras Fault Zone, and NW-SE trending normal faults, the last ones controlling the tilting towards the east.

An earthquake segmentation of the CFZ cannot be established since no historical or instrumental seismicity can be univocally associated with it. Fault segmentation is proposed in line with geomorphological and structural observations. Two scales of structural segmentation are put forward. First-order segments are defined on the basis of morphology (i.e. changes in the fault trace orientation), and second-order segments were defined on the basis of variations in the fault structure in its upper-most kilometres. Two first order segments are defined: the N047º/050º trending North Carboneras Fault (NCF) segment and the N059º/050º trending South Carboneras Fault (SCF) segment. This change in the fault trace orientation is thought to be caused by the interaction of the fault zone with an oblique shear zone in the SE part of the SCF. Seven second order sub-segments are differentiated along the NCF segment and 3 along the SCF segment.

These are characterized by from north to south: NCF-d) a complex wide fault zone, NCF-c) a narrower fault zone, NCF-b) two parallel fault traces forming a flower structure at depth, NCF-a) a single trace with poor surface expression, NCF-1) a positive flower structure, NCF-2) a vertical fault zone forming a pressure ridge, NCF-3) a N047º trending narrow vertical fault zone, SCF-4) a fault zone with prominent pressure ridges, SCF-5) a N059º trending narrow vertical fault zone, and 6) a N050º trending narrow vertical fault zone. The sub-segment boundary between NCF-1 and NCF-a is placed at the shore-line for practical reasons and lacks structural meaning. Further analysis in this part of the CFZ should be carried out.

The segments and sub-segments described for the CFZ do not necessarily represent the fracture arrest during an earthquake. However, these structural changes could pose a problem for the transmission of the rupture. Thus, maximum magnitudes of each of these segments and sub-segments are estimated on the basis of their length using the Wells and Coppersmith (1994) empirical relationships. Second order segments yielded maximum magnitudes ranging between Mw 6.1 +/-0.2 (NCF-a sub-segment) and Mw 6.7 +/-0.3 (NCF-3 sub-segment). First order segments yielded maximum magnitudes of Mw 7.4 +/-0.3 for the NCF segment, and Mw 7.0 +/-0.3 for the SCF segment. The worst case scenario would be the complete rupture of the CFZ, which would produce a maximum magnitude of Mw 7.6 +/-0.3. Another approach used to estimate the maximum magnitude was from the maximum 1.5 m slip per event inferred from the offset paleo-channel (NCF-b sub-segment), suggesting a maximum magnitude of Mw 6.9-7.0. This is a lower value than that calculated for the entire NCF segment and suggests that 1) the earthquake during which the paleo-channel was offset does not represent the maximum earthquake along the NCF segment; 2) the NCF segment is divided into shorter segments with independent seismic personality; and 3) the strain released during that event was distributed along several fault traces, and thus the offset measured at El Hacho has a minimum value.

Strike-slip rates where calculated along the fault trace. Minimum results range between 0.05-1.3 mm/yr for different periods of time. However, better constraints of these results can be obtained by combining geological and geodetic data (preliminary GPS results). A minimum strike-slip rate of 1.3 mm/yr was estimated for the Northern Carboneras Fault segment along the Quaternary. This represents at least 23.2% of the total shortening between the Eurasian and African plates.

Dip-slip rates measured along the CFZ show a large variety of results (0.01-0.3 mm/yr for different periods of time) probably a) because the fault is strike-slip and laterally offsets irregular topography and b) because there are variations along the fault trace according to the tilting sub-block model on the northwestern wall of the CFZ. These values, however, strongly suggest that the dip-slip component of the fault is one to two orders of magnitude lower than the strike slip component.

Trenching analysis provided evidence of a minimum of 5 events at El Hacho (E1: 130-49.9 ka BP, E2: 130-49.9 ka BP, E3: 41.5-26.6 ka BP, Ea: 32.1 ka BP-AD 934 and Eb: AD 775-Present day) and 4 events at Los Trances (L1: 191-130 ka BP, L2: 191-130 ka BP, L3: 83-59.5 ka BP and L4: 71-0 ka BP). Some events at the two sites can be correlated and thus a minimum of 7 events since 191 ka suggest a mean recurrence period of 27.3 ka. Taking into account the last three events since 41.5 ka BP the mean recurrence period decreases to 13.8 ka. However, the recurrence period might be probably one order of magnitude lower, about 1.1 ka, according to the slip-rate (>1.3 mm/yr) and the slip per event (≤1.5 m). The apparent close-in-time occurrence of the two last events, inferred from geomorphological interpretations, lends support to this interpretation.

The CFZ, which is characterized by a lack of historical and instrumental seismicity, was demonstrated to be a seismogenic structure capable of generating large magnitude earthquakes. Therefore, its seismic potential should be taken into account in the seismic hazard assessment of the Iberian Peninsula. This highlights the need for further paleoseismic analysis in the region to detect other structures, which like the CFZ, lack historical and instrumental seismicity but could be potential seismogenic structures. The integrated onshore-offshore analyses carried out in this study offers valuable insights into the seismic potential of the CFZ. The paleoseismic parameters obtained are summarized below and will contribute to active fault databases providing more realistic values for further seismic hazard modelling and assessment.

- ✓ Age of youngest deposits affected: AD 775-934
- ✓ Vertical slip rate: >0.01 mm/yr and <0.3 mm/yr for different periods of time from the Pliocene to the Holocene
- ✓ Horizontal slip rate: >1.1-1.3 mm/yr for different periods of time from the Pliocene to the Holocene
- ✓ Net slip rate: >1.1-1.3 mm/yr
- ✓ Max slip/event: ≤1.5 m
- ✓ Number of seismic events observed: ≤7 events since 191 ka BP
- ✓ Recurrence interval: about 1.1 ka
- ✓ Max magnitude (Mw): 6.9-7.6 +/-0.3